Exp Brain Res (2007) 178:402–414
DOI 10.1007/s00221-006-0751-9

RESEARCH ARTICLE

Motor adaptation to a small force field superimposed on a large background force

Jiayin Liu · David J. Reinkensmeyer

Received: 9 December 2005 / Accepted: 6 October 2006 / Published online: 8 November 2006

Abstract The human motor system adapts to novel force field perturbations during reaching by forming an internal model of the external dynamics and by modulating arm impedance. We studied whether it uses similar strategies when the perturbation is superimposed on a much larger background force. Consistent with the Weber–Fechner law for force perception, subjects had greater difficulty consciously perceiving the force field perturbation when it was superimposed on the large background force. However, they still adapted to the perturbation, decreasing trajectory distortion with repeated reaching and demonstrating kinematic after effects when the perturbation was unexpectedly removed. They also adapted by increasing their arm impedance when the background force was not present, but did not vary the arm impedance when the background force was present. The identified parameters of a previously proposed mathematical model of motor adaptation changed significantly with the presence of the background force. These results indicate that the motor system maintains its sensitivity for internal model formation even when there are large background forces that mask perception. Further, the motor system modulates arm impedance differently in response to the same perturbation depending on the background force onto which that perturbation is superimposed. Finally, these results suggest that computational models of motor adaptation will likely need to include force-dependent parameters to accurately predict errors.

Keywords Motor skills · Learning · Perception · Arm movement

J. Liu · D. J. Reinkensmeyer (✉)
Department of Mechanical and Aerospace Engineering, University of California, 4200 Engineering Gateway, Irvine, CA 92697-3975, USA
e-mail: dreinken@uci.edu

D. J. Reinkensmeyer
Department of Biomedical Engineering, University of California, Irvine, CA, USA

Introduction

The human motor system has the ability to adapt to novel environments based on previous experiences. A number of studies have investigated the strategies used to improve motor performance with repetitive practice. One of the essential findings is that the motor system can form ''internal models'' of limb dynamics and external loads and predictively compensate using these models in a ''feed-forward'' control mode. Existence of internal models has been demonstrated for several motor tasks, including reaching (Shadmehr and Mussa-Ivaldi 1994; Gandolfo et al. 1996; Shadmehr and Brashers-Krug 1997), drawing (Conditt et al. 1997), and walking (Emken and Reinkensmeyer 2005). A useful experimental paradigm in these studies has been to use robot manipulators to generate novel dynamic environments, or ''force fields'', during these tasks. When subjects are first exposed to a force field, their limb trajectories are distorted in the direction of applied force compared with the limb path under the normal dynamic environment. After continuous exposure, subjects gradually adapt to the new dynamic environment, and the limb movements shift toward the original trajectories. When the force field is unexpectedly removed after the adaptation occurs, movement

trajectories become distorted in the opposite direction of the applied force field. Such anticipatory control based on a model of the field's action is beneficial for producing fast and coordinated movements, since biological feedback loops are slow.

It is currently unknown how the motor system's sensitivity for forming internal models of perturbations varies with the force regime in which the perturbations operate. Most experiments have been done with an experimental paradigm in which subjects experience a sudden switch between no force field (i.e., a ''null field''), and a novel force field, the strength of which is small relative to the subject's strength. The novel force field is generated by a robot manipulator, and is easy for subjects to consciously detect. There are known physiological mechanisms, however, which suggest that adaptation might be different when the force field is superimposed on a larger background force. For example, Weber–Fechner's law (Weber 1846) describes how the sensitivity of force perception varies with the background force: the just noticeable difference for detecting a weight change varies in proportion to the weight on the hand. Jones (1989) further showed that the Weber fraction was 0.07 for force perception, that small forces were consistently overestimated, and that the most accurate estimation occurred in the middle of the force domain (Jones and Hunter 1982). Internal model formation depends on error sensing, and computational models of motor adaptation have been proposed in which errors are expressed as perceived and expected forces (Thoroughman and Shadmehr 2000). If the sensitivity of error sensing degrades with larger background forces according to the Weber–Fechner relationship, then internal model formation may be impaired at larger forces. To test this possibility, we studied the ability of subjects to adapt to a small force field when the force field was superimposed on a much larger background force

A second strategy used by the motor system to adapt to novel dynamic environments is impedance control. The motor system purposely modulates impedance in the early stages of internal model learning (Milner and Franklin 2005) and in unstable (Burdet et al. 2001) or unpredictable environments (Takahashi et al. 2001b). Evidence also showed that the strategies of internal model formation and impedance control can be used simultaneously during adaptation to small force fields (Takahashi et al. 2001b; Osu et al. 2003; Milner and Franklin 2005). Further, a computational model has been proposed to describe how joint torque and impedance are modulated when adapting to small force fields, based on kinematic error and sensed endpoint force (Burdet et al. 2005). A potentially confounding factor when using impedance control to adapt to disturbances that are superimposed on large background forces, however, is that arm stiffness increases with arm force, due to the obligatory coupling of muscle stiffness with muscle activation related to crossbridge formation. A stiffer arm will respond with a smaller error to the same force perturbation. Thus, we hypothesized that purposeful changes in arm impedance may not be necessary in the presence of a large background force.

To examine these issues, we compared how people adapted to the same small force field when it was superimposed on either a zero background force or a much larger background force that was applied in the same direction as the force field's action. We quantified internal model formation using catch trials to reveal aftereffects of adaptation. We assessed changes in arm impedance by unexpectedly changing the force applied to the arm, and measuring the resulting trajectory deviation. Finally, we analyzed whether the parameters of a previously proposed mathematical model of motor adaptation (Liu and Reinkensmeyer 2004; Emken and Reinkensmeyer 2005) varied with the level of background force. Portions of this work have been reported in conference paper format (Liu and Reinkensmeyer 2004).

Methods

Experimental protocol

Twelve subjects (10 M, 2 F, ages 23–37) with no known sensory motor impairments participated in the study, which was approved by the U.C. Irvine Institutional Review Board. Subjects sat in a chair with a harness to constrain trunk motion. The subject held the tip of a lightweight robot arm (PHANToM 3.0, SensAble Technologies, Inc.) that was free to move in three dimensions with the right hand (the dominant hand for each subject) and reached between a ''start'' target, positioned two hand widths out from the sternum, and a ''finish'' target, positioned just inside the boundary of the reaching workspace and aligned with the start target directly in front of the subject at the same height (Fig. 1a). In each trial, the subject tried to reach at the same speed. A pre-test consisted of 20 fast-as-possible reaches, and the desired time was set to be 118% of the mean of the reach times of the fastest three trials (i.e., 85% of mean speed). Feedback of the reach duration (just right = desired reach time ± 5%; too fast; or too slow) was provided after each movement to help subjects maintain a constant speed. Thus, subjects

reached briskly, but not as fast as possible. Typical movement lengths were about 30–35 cm, and typical movement durations about 1 s.

While performing this reaching task subjects adapted to a viscous curl field, with and without a side load applied to the arm. The viscous curl field was:

$$F = k \cdot b \times v, \quad (1)$$

where $k \in \{-1, 1\}$ (force field direction), $v = [v_x \; v_y \; v_z]^T$ m/s (velocity of subject's hand), and $b = [0 \; 3.65 \; 0]^T$ N s/m (in this case, force is perpendicular to velocity), with x being to the right, y straight up, and z toward the subject in the forward-backward direction (Fig. 1a). The resulting force, applied only during the outward reach, was either leftward ($k = 1$) or rightward ($k = -1$). The peak magnitude of the force field, averaged across subjects was 3.3 ± 0.8 N. This velocity-dependent force field, which has been used in many previous adaptation experiments (e.g., Shadmehr and Mussa-Ivaldi 1994; Gandolfo et al. 1996; Goodbody and Wolpert 1998), was used here because it guarantees zero force before subjects begin to move, and prevents them from predicting whether the force field will be ''on'' for the next reach. Since the subjects tried to keep their speed constant, the forces applied were similar between trials.

We desired to measure adaptation to the force field when it was superimposed on a much larger background force that operated in the same direction. The robot was too weak to produce the desired large load, so a side load was provided by an elastic band (Medicordz). The band was attached between a wrist strap and a pedestal in front and to the left of the subject at approximately the same height as the targets (Fig. 1a). The stiffness of the elastic band was approximately 105 N/m at the lengths it was used. The side load was leftward directed at approximately the vertical level of the reach. For reaches in a straight line from the start to finish targets, the magnitude of the side load varied from 30 to 60 N, with the minimum value near the end of the reach. Thus, the side load was approximately 10–20 times stronger than the force field perturbation. The strength of the side load was chosen to be as large as possible while still allowing subjects to complete the reaching task with a level of fatigue that was manageable with periodic, short breaks. These side forces were approximately 30% of the average adult strength in this direction, as measured in a previous experiment with a similar experimental set-up (Takahashi et al. 2006). Subjects were able to see the elastic band when it was attached. They were given 40 reaches to accommodate to reaching with the side load before they adapted to the force field.

Subjects adapted to the viscous force field with the side load absent or present, and within each of these conditions, they adapted once with the force field directed leftward and once with it directed rightward. There were 140 reaches for each of the resulting four adaptation tests (Fig. 1c). The order of the four adaptation tests was randomized. For tests with a side load, the side load was set up at the beginning of each test and stayed either present or absent for the entire duration of the test.

The 140 reaches for each adaptation test were divided into three phases (Fig. 1c). We will refer to the first phase of 40 reaches as the ''baseline'' phase during which subjects practiced reaching, accommodating to the background load condition. The robot force field was turned ''off'' most of the time during the baseline

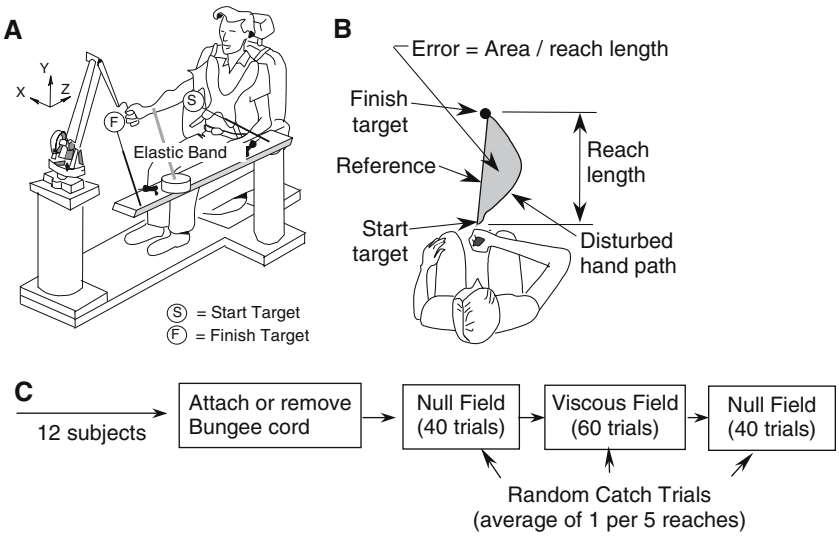

Fig. 1 Experimental protocol. **a** Subjects moved a lightweight robotic manipulator between a start and finish target with or without a side load created by an elastic band attached to their wrist. The targets were positioned at the same height, typically 30–35 cm apart. **b** Reaching error was defined as the spatial average lateral deviation away from a straight line between start and finish target. **c** Subjects adapted to a viscous curl field, applied by the robot, with or without the side load

phase, except for ''catch trials'' during which the force field was unexpectedly toggled on for the reach. These catch trials were interspersed with an average period of five trials through the whole experiment. Subjects then performed 60 reaches in the viscous force field to measure adaptation (the ''adaptation phase''). They then performed 40 reaches in a ''washout phase'' during which the robot force field was again ''off'' except for catch trials.

To manage fatigue in the side loaded condition, subjects rested after every 20 trials for 40 s, starting at trial 10. These rests breaks were also given during the non side-loaded condition to keep the adaptation test the same except for the side load. The spacing of the rest breaks was chosen so that there were no rest breaks immediately before or after key transitions in the protocol (e.g., the transition from baseline phase to adaptation phase was not interrupted by a rest break.)

Subjects had difficulty perceiving the force field when the side load was applied. We quantified this effect in a second experiment with the same subjects by randomly modulating the force field gain used for each reach by a multiplier chosen from the set {–1.0, 0.5, 0.0, 0.5, 1.0}, and asking the subjects to identify whether the robot pushed them full strength right, half right, not at all, half left, or full left. The subjects reached 50 times in this paradigm, with and without the side load, and always with vision of the arm. We measured the field perception for all 12 subjects, but recorded reaching trajectories from only five of the subjects during this experiment.

Data analysis

A computer sampled the three-dimensional position of the robot tip (and thus the subject's hand position) at 200 Hz, as inferred from rotational sensors at the robot joints. The force field was designed to push the hand to the left or right, so disturbances to the reaching trajectory were mainly in the horizontal plane. Thus, we quantified reaching errors as the area between the trial path and a reference path projected onto the horizontal plane (x–z-plane, Fig. 1a), divided by the distance between the start and finish targets (Fig. 1b). The resulting geometric measure of error is a spatial average lateral deviation away from the reference path (Takahashi et al. 2001b), which we will refer to as ''average lateral deviation'' or ''reaching error''. We chose this measure to quantify error instead of maximum deviation because it is influenced explicitly by the whole trajectory, rather than by just the peak deviation point of the trajectory, and thus has averaging properties that reduce trial-to-trial noise. We chose it instead of time-averaged deviation because the hand spends more time near the start and end of the reach, biasing time-averaged error measures to these early and late parts of the trajectory that are less sensitive to the effect of the velocity-dependent force field. We gave reach paths that were to the left of the reference path positive values, and those to the right negative values. We selected the reference path to be a straight line between the start and finish targets.

To characterize adaptive performance, we calculated several measures based on reaching error. Baseline reaching error was defined as the mean of the error on the last 15 non-catch trials in the baseline. The error was approximately constant during the last part of the baseline phase, as subjects had adapted to the presence or absence of the elastic band (Fig. 3). Initial error (Fig. 4a) was defined as the reaching error for trial 41 (i.e., at the start of the 60 trials with the force field) minus the baseline reaching error. Final error (Fig. 4a) was defined as the average reaching error of the last five non-catch trial reaches in the force field, referenced to the baseline error. We calculated after-effect size (Fig. 4b) as the reaching error on catch trials during the later part of force field exposure (reaches 60–100), again referenced to the baseline reaching error. Statistical analysis of the adaptive performance measures was done primarily using paired t-tests, comparing loading conditions, with a significance level of 0.05, adjusted with the Bonferroni correction in the case of multiple comparisons.

Previous research has indicated that internal models are rapidly updated in response to changing environments (Thoroughman and Shadmehr 2000). To examine any rapid de-adaptation due to catch trials, we calculated the change in reaching error on the 4 trials following each catch trial, relative to the reaching error on the trial immediately before the catch trial ($\Delta e_{ct+i} = e_i - e_{ct}$, $i = 1, 2, 3, 4$, Fig. 4d). We included catch trials from the baseline phase, the force field phase, and the washout phase, starting with the fourth catch trial in each section to eliminate the effects of the changing baseline due to adaptation/de-adaptation.

To quantify limb impedance, we measured the change in reaching error that resulted during catch trials. Since the change in force during a catch trial was always a constant magnitude, then the change in reaching error due to this change in force is a gross measure of the limb impedance throughout the reach. This measure includes the effects of muscle stiffness and, later in the reach, reflex contributions to arm impedance. We used the reaching error on the most recent reach as the reference value for calculating the change in reaching error due to a catch trial on the next

reach (Δe_{ct}, Fig. 5). That is, we analyzed the differential change in movement trajectory caused by a differential change in force, as a gross measure of impedance throughout the movement.

Computational model of motor adaptation

We were also interested in whether current modeling approaches to force field adaptation are effective in modeling error evolution under the disparate force regimes studied here. Previous studies have shown how the evolution of kinematic error during motor adaptation is well described by a simple, linear difference equation (Thoroughman and Shadmehr 2000; Scheidt et al. 2001a; Emken and Reinkensmeyer 2005):

$$x_{i+1} = a_0 x_i + b_1 F_i + b_0 F_{i+1} + c_o, \tag{2}$$

where x_i is the kinematic reaching error on the ith reach, F_i is the average lateral force from the viscous force field on the ith reach, and a_0, b_1, b_0, and c_0 are constant coefficients. The parameters of this equation can be identified using multiple linear regression on the sequence of forces applied and errors experienced during adaptation. We compared the ability of this equation to model adaptation to the force field with and without the side load.

Equation 2 does not separate out the mechanical effects of the force field and limb impedance from the neurocomputational mechanisms that underlie motor adaptation. We recently showed how Eq. 2 can be viewed as arising from the interaction of an error-based learning law with the limb/force field dynamics (Liu and Reinkensmeyer 2004; Emken and Reinkensmeyer 2005). We assume that the arm behaves like a spring in response to external and muscle forces in the medial–lateral directions, when movements in these directions are limited to a small range, so:

$$x_i - x_d = \frac{1}{K}(F_i + u_i), \tag{3}$$

where x_i is the average lateral deviation from a straight line on the ith reach, x_d is the average lateral rest-length of the spring, F_i is the average lateral force from the viscous force field on the ith reach, u_i is the average lateral force from the arm on the ith reach, and K is the arm stiffness. The variables x_i, F_i, and u_i are all defined positive to the right. The assumption of spring-like behavior is supported by the observation that reaching error varied approximately linearly with field strength during catch trials when the viscous curl field was applied, for reaching with and without the side load (Fig. 6c). When the side load was applied, we also use Eq. 3 to model the error dynamics of the task, because in this situation the arm produced a ''tonic'' force equal and opposite to the side load in order to move toward the target again. In this situation, u_i is the change in arm force, referenced to this tonic arm force that is created to compensate for the viscous force field perturbation F_i. For the following derivation, we also assume K is constant.

The proposed learning law is:

$$u_{i+1} = f u_i - g(x_i - x_d), \tag{4}$$

where $f \leq 1$ is a ''forgetting factor'', g is the ''learning gain'', and x_d is the desired kinematic performance, which we assume is constant for the entire section of 140 movements. One way to view this learning law is that the nervous system increments the motor command in proportional to the previous error, in the direction that will reduce the error. If $f < 1$, then the nervous system increments a decremented version of the previous motor command due to ''forgetting''. The learning gain g determines how much the internal model is adjusted based on the previous movement error, and influences the speed and stability of convergence of the algorithm. This learning law can also be expressed equivalently using force errors to drive it by substituting the expression for x_i from Eq. 3 into 4:

$$u_{i+1} = f u_i - g^*(F_i - u_d), \tag{5}$$

where $g* = \frac{g}{K}$ is a unit-less learning gain. Here, F_i is the external force applied, and $u_d = -u_i$ is the external force expected to be applied to the arm on the ith reach. This formulation is similar to recently proposed learning models (Thoroughman and Shadmehr 2000; Donchin et al. 2003), except that it includes a forgetting factor, similar to (Burdet et al. 2004).

Combining Eqs. 3 and 4 (see Emken and Reinkensmeyer 2005), the evolution of the lateral deviation x_i, measured with respect to the straight line, s:

$$x_{i+1} = \left(f - \frac{g}{K}\right)x_i - \frac{f}{K}F_i + \frac{1}{K}F_{i+1} + \left(1 - \left(f - \frac{g}{K}\right)\right)x_d, \tag{6}$$

which is of the same form as Eq. 2. The learning parameters f, g, K, and x_d can be calculated from the regression coefficients from Eq. 2 as follows:

$$K = \frac{1}{b_0} \quad f = -\frac{b_1}{b_0} \quad g = K(f - a_0) \quad x_d = \frac{c_0}{1 - a_0}. \tag{7}$$

We examined how the parameter K, which is the limb/environmental stiffness, and the parameters f, $g* = \frac{g}{K}$, and x_d, which are the parameters of the putative error-based learning law, varied during motor adaptation with and without the side load.

Results

Subjects adapted to the robot-generated, viscous, curl field while reaching to a target in two conditions: with or without a background, elastic, side load that was about ten times larger than the viscous field itself. Figure 2 shows typical reaching trajectories from one subject for the case in which the force field pushed to the right (the elastic bands, when present, always pulled to the left). The reaching trajectory was roughly straight during the baseline phase when the force field was not applied, with and without the side load. When the viscous field was applied, it perturbed the reaching trajectory significantly to the right. In both loading conditions, the subject adapted to the force field during the adaptation phase, and the reaching trajectory shifted back to the left toward the baseline trajectory (gray continuous lines in Fig. 2). The subject exhibited an aftereffect when the viscous field was unexpectedly removed during catch trials in both conditions, moving to the left of the original baseline trajectory (gray broken lines in Fig. 2).

To quantify the distortion of reaching trajectory during adaptation, we examined the average reaching error across the 12 subjects. In both loading conditions, when the field was turned on at trial 41, subjects exhibited a significant initial error (Figs. 3, 4a). This initial error was smaller in the side-loaded condition (Fig. 4a), as would be expected since the elastic bands added stiffness to the arm, and also since muscle stiffness increases with activation level (McIntyre et al. 1996; Gomi and Osu 1998). The subjects adapted to the force field and reduced their reaching error with practice in both loading conditions, but the final reaching error was significantly smaller during side loading (Figs. 3, 4a, $P < 0.01$, paired t-test).

The subjects also generated significant after-effects when the field was unexpectedly removed following adaptation during catch trials in both conditions, suggesting that they had learned to predict the field ($P < 0.01$, t-test comparing after-effect size to zero, Fig. 4b). The after-effect sizes were smaller during side loading ($P < 0.01$, paired t-tests), again likely due to the stiffness increases arising from the elastic bands and the muscle force-stiffness dependence. The ratio of the after effect size to the direct effect size were not significantly different between conditions (Fig. 4c).

The subjects responded differently during the reaches that immediately followed the catch trials, depending on the loading condition. During reaching without the side load, catch trials caused a partial

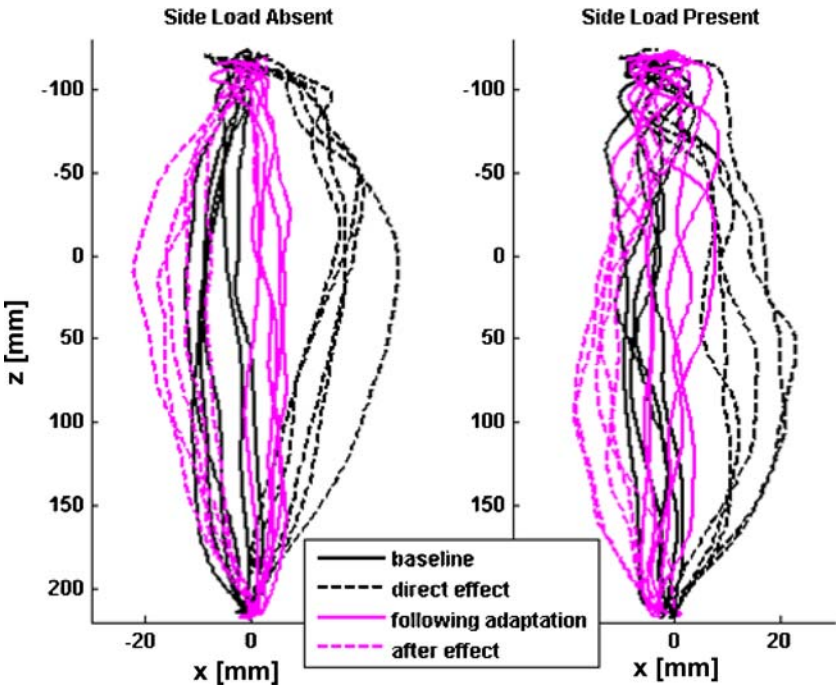

Fig. 2 Hand trajectories in horizontal plane from one subject. *Black continuous line*: baseline, last 5 non-catch trials in baseline phase; *black broken line*: direct effect, last 5 catch trials in baseline phase; *gray continuous line*: following adaptation, last 5 non-catch trials in force field phase; *gray broken line*: after effect, last 5 catch trials in force field phase; *left*: side load absent condition; *right*: side load present condition. Please note that the scales in the x and y directions are different to make the trajectory curvature more visible

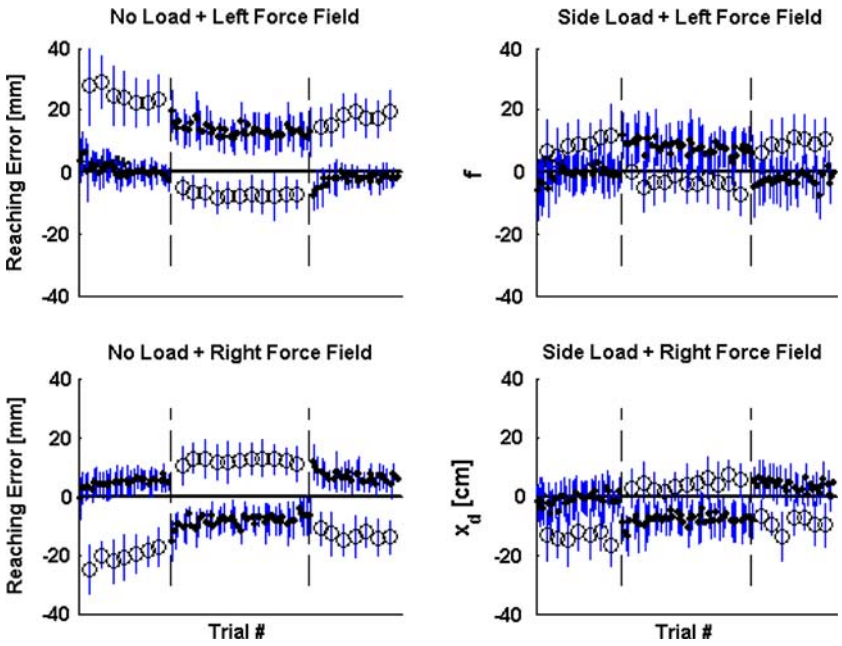

Fig. 3 Average reaching error across 12 subjects. Four loading conditions are presented: side load absent/present; force field to the left/right. Positive error is defined as moving left to the reference line. Catch trials are presented by *circles*, and other trials are presented by *dots*. *Bars* are standard deviation across 12 subjects

de-adaptation followed by a rapid re-adaptation, as has been observed before (Fig. 4d) (Thoroughman and Shadmehr 2000). For example, if a catch trial was given during adaptation to the viscous force field (i.e., the force field was unexpectedly turned off), then the reaching error on the first trial after the catch trial was

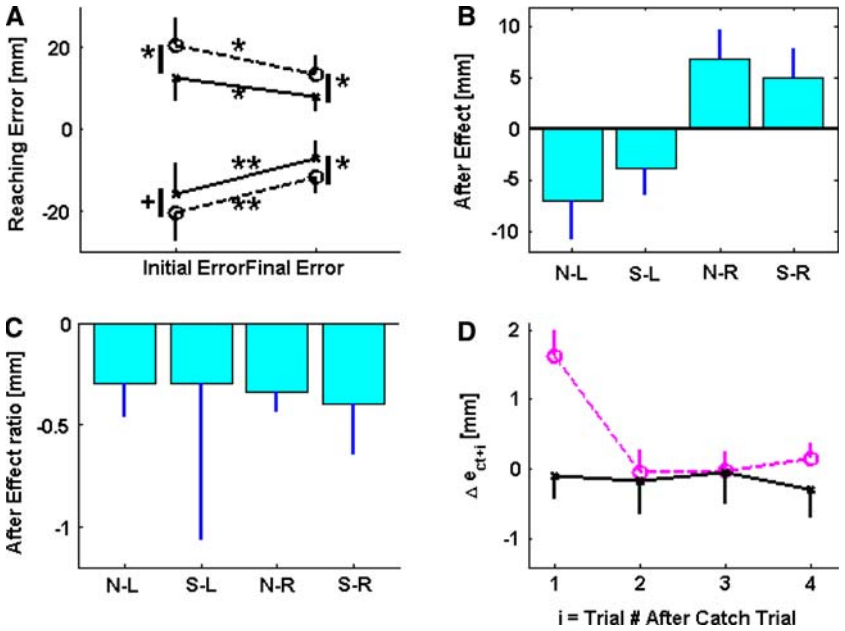

Fig. 4 Measures of adaptation. The means in panels **a**–**c** are across subjects, and the *error bars* show ± one standard deviation across subjects. **a** Initial and final reaching errors, without (*open circle*) and with (*crosses*) the side load for the leftward (*top lines*) and rightward force fields (*bottom lines*). $^{**}P < 0.001$, $^{*}P < 0.01$, $^{+}P < 0.1$, one side paired *t*-tests. **b** After effects during catch trials after adaptation were significantly different from zero for all four loading conditions ($P < 0.05$, *t*-test, 12 subjects). After effects were significantly smaller with side loading ($P < 0.001$). *S, N* side load, no side load; *L, R* left force field, right force field. **c** The after effect ratio was not different between loading conditions. The after effect ratio is calculated by $\frac{\text{After Effect Size}}{\text{Direct Effect Size}}$ **d** Change in reaching error following a catch trial (Δe_{ct+i}) without (*open circle*) and with (*crosses*) side load, relative to reaching error immediately prior to the catch trial. The sign of Δe_{ct+i} was referenced to the direction of the force change for the catch trial

larger than the reaching error on the trial just before the catch trial, with the error decaying rapidly with further practice. During side loading, however, catch trials apparently did not cause a transient de-adaptation (Fig. 4d).

Arm impedance was modulated differently during the two conditions also, as quantified by the kinematic error incurred during catch trials, measured relative to the reach path from the reach immediately preceding the catch trial (Fig. 5). The magnitude of this differential kinematic error ($|\Delta e|_{ct}$) is dictated by the arm impedance throughout the movement; a stiff arm would allow only a small $|\Delta e|_{ct}$ in response to the changed force on the catch trial. During reaching with no side-load, $|\Delta e|_{ct}$ decreased significantly over the first 60 reaches ($P < 0.001$; paired t-test across subjects comparing $|\Delta e|_{ct}$ for first catch trial to its mean across last ten catch trials), indicating an increase in arm impedance with practice (Fig. 5). During side loading, $|\Delta e|_{ct}$ was smaller due to the increased stiffness of the limb and the elastic cords, and did not change significantly ($P = 0.15$; Fig. 5).

Presence of the side load also reduced the subjects' ability to perceive the force field. Subjects reported that they were not aware of the robot-generated perturbation most of the time in the side load condition. We quantified this effect in a second experiment in which subjects verbally reported the field strength as it varied randomly from reach to reach, although they were not confident in side load condition. They accurately estimated the field strength when there was no side load (Fig. 6a), but inaccurately guessed that the field was not applied about 50% of the time when the side load was present, for the viscous field strengths used in the adaptation experiments (Fig. 6b). They accurately guessed both the force field strength and direction 18% (±23% SD across subjects) of the time for the full strength field (i.e., about chance level: 1 in 5).

We used multiple linear regression across 140 movements in each condition to fit a previously-described mathematical model of motor adaptation (i.e., Eq. 2) to the experimental data. The linear regressions were highly significant for both conditions across the task ($P < 0.0001$ for all regressions). The r^2 value was lower in the side-loading condition (mean $r^2 = 0.51$ across subjects) compared to no load (mean $r^2 = 0.83$). This drop was caused at least in part by greater randomness in the reach trajectories in the side-loaded condition, as the mean trial-to-trial variability in reaching error was 2.9 cm ± 0.9 SD during free reaching and 4.8 cm ± 0.7 SD during side loading, a significant difference ($P < 0.01$, paired t-test).

The regression constants a_0, b_1, and b_0 decreased significantly in the side loaded condition (t-test, $P < 0.0001$ for both b_1 and b_0, Fig. 7). Significant differences were also found in the parameters of the error-based learning model (Eq. 6, Fig. 8), which were calculated from the regression coefficients using Eq. 7. Specifically, the forgetting factor f decreased significantly with side load ($P < 0.01$). The modeled limb/environment stiffness K increased significantly with side load ($P < 0.0001$) as would be expected.

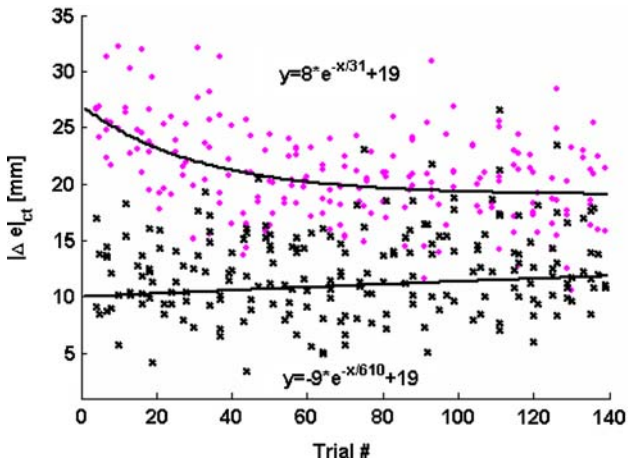

Fig. 5 Magnitude of change in reaching error ($|\Delta e|_{ct}$) caused by catch trials without (*dot*) and with (*crosses*) side load. Data for the left and right force field directions for all subjects are combined for each loading condition. The best-fit exponential curves are shown

Discussion

A primary finding of this study was that subjects retained the ability to form an internal model of a small, force field perturbation when that perturbation was unexpectedly superimposed on a much larger background force. They retained this ability even though conscious awareness of the force field was severely impaired by the much larger background force. Thus, the core adaptation mechanism of internal model formation was operational within a force regime very different than the one that has been examined in previous research studies, even though force perception changed dramatically in this regime. Another key finding was that the subjects' use of impedance control (i.e., how they modulated arm impedance throughout the course of the repeated exposure to the force field) differed depending on the presence of the background force. Finally, the parameters of two mathematical models used previously to describe motor adaptation

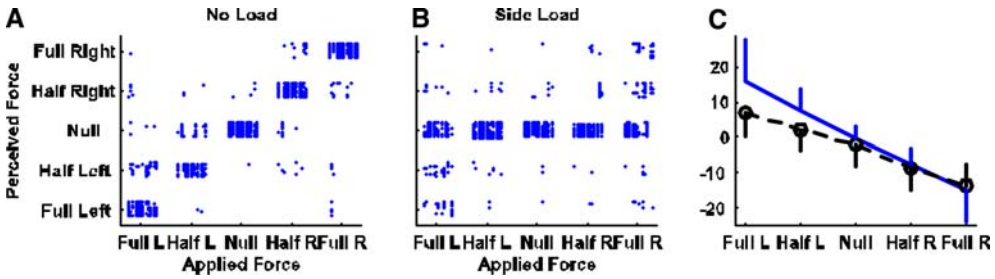

Fig. 6 Perception of the force field in unloaded and side-loaded conditions. **a** Perception without side load. Each column of dots represents data from a single subject, and each dot a single reach. **b** Perception with side load. **c** Average perturbation size for different field strengths for five subjects with (*sold line*) and without (*dashed line*) side load. Here, the error bars are the mean across subjects of the 95% confidence intervals for the reaching error

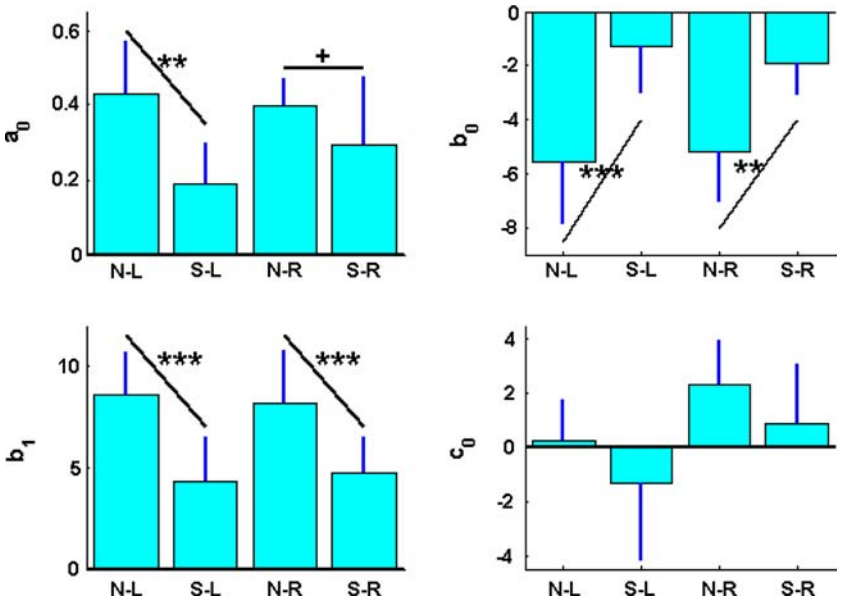

Fig. 7 Regression constants for the motor adaptation model described by Eq. 1. Each panel shows average regression constants and standard deviation across subjects in the four loading conditions. *S, N* side load, no side load; *L, R* left force field, right force field. The parameters b_1 and b_0 decreased significantly in the side loaded condition (paired *t*-test, $P < 0.0001$ for b_1, $P < 0.006$ for b_0), while the decrease in a_0 neared significance ($P < 0.1$). $^{***}P < 0.0001$, $^{**}P < 0.001$, $^{+}P < 0.1$

changed significantly when the background force was present.

Internal model formation in the presence of a large background force

The motor system was still able to adapt to the small force field when it was unexpectedly superimposed on the large, elastic force: subjects exhibited an initial error when the force field was first applied, then movement error decreased with repeated training, and then subjects generated an opposite kinematic error when the force field was unexpectedly removed after the adaptation occurred. The presence of the after effect is evidence that the motor system used anticipatory control based on the immediately preceding experience of the superimposed force field. Thus, the motor system adjusted its internal model of the overall environment in response to a differential change added to or subtracted from an already large force; i.e., it was sensitive to small force changes away from the larger, continuous forces that it was required to generate.

Subjects had difficulty judging the force field strength during the side-loaded condition. Thus, this study showed that force perception during movement in a force field is consistent with Weber–Fechner's law, which is typically studied in isometric conditions, and which posits a linear relationship between perception

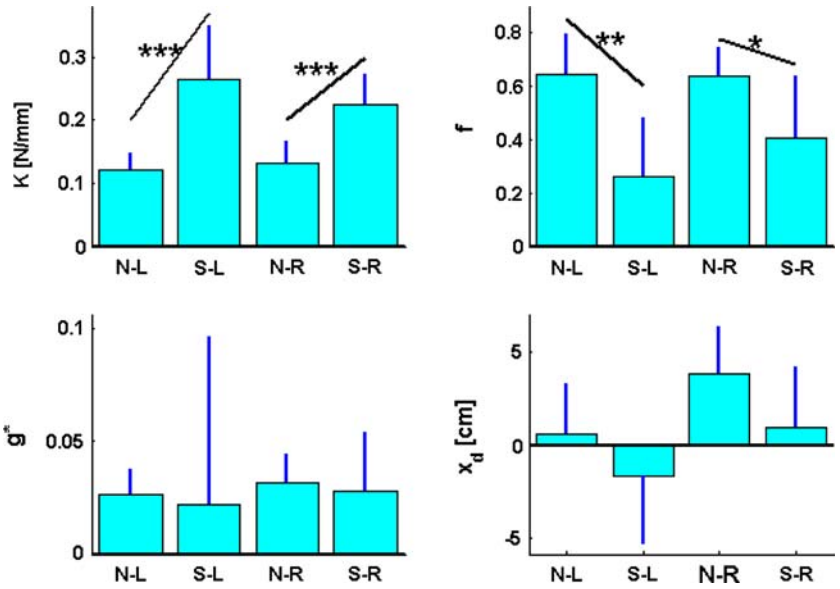

Fig. 8 Identified parameters of the motor adaptation model described by Eqs. 2 and 3. Each panel shows average identified parameters and standard deviation across subjects in four loading conditions. K limb/environment stiffness, f forgetting factor, g^* learning gain, x_d desired trajectory. *S, N* side load, no side load; *L, R* left force field, right force field. The forgetting factor f decreased significantly with side load (paired t-test, $P < 0.01$). The limb/environment stiffness K increased significantly with side load ($P < 0.0001$). $^{***}P < 0.0001$, $^{**}P < 0.001$, $^{*}P < 0.01$

of a change of force and the overall force applied. More recent studies pointed out that the relationship is not linear when the force is small, but that there was always a positive correlation between the change in force required for perception and the overall applied force (Jones 1989). In previous studies of force field adaptation (e.g., Shadmehr and Mussa-Ivaldi 1994; Gandolfo et al. 1996; Conditt et al. 1997; Shadmehr and Brashers-Krug 1997; Takahashi et al. 2001b), the presence of the force field was consciously detectable because it was always introduced following reaching with no external forces. The results of this study suggest that precise, conscious error sensing and awareness of the perturbation are unnecessary to form an internal model. Thus, we propose that the process of internal model formation is dissociated from conscious awareness of the force field.

It is well known that motor systems respond to subconscious sensory information, for example, to maintain balance in response to visual and vestibular inputs. Skilled motor actions have also been shown to respond to subconscious perception in healthy and brain-damaged subjects (Goodale et al. 1991; Rossetti et al. 1995; Imanaka et al. 2002; Brewer et al. 2005; Johnson and Haggard 2005). In a classic example of dissociation of motor performance and perceptual awareness, subjects were asked to make rapid pointing movements toward a small visual target, without vision of the hand (Pelisson et al. 1986). The target was unexpectedly moved slightly during a saccade, which suppressed visual information processing (Shioiri and Cavanagh 1989). Without noticing the target location had been changed, subjects smoothly adjusted their reaching movement corresponding to the new target. Another example is the adaptation of motor response of finger tapping to the unperceived frequency change of a metronome (Thaut and Kenyon 2003; Repp 2004). Motor adaptations without perceptual awareness during reaching movements were demonstrated when subjects adapted to slowly shifted vision feedback of each reach by shifting their actual arm trajectory without awareness (Goodbody and Wolpert 1999), or a slowly changing force field (Klassen et al. 2005). These findings imply that motor processes and conscious perceptual processes often take place in parallel rather than in series (Willingham 2001). Consistent with these previous findings, our results suggested a dissociation between motor adaptation and conscious perception for the task of learning an internal model of a novel force field.

It is possible to draw an analogy between the present experiments and masking experiments, which suppress the perception of a small testing stimulus by a large masking stimulus. For example, a backward mask consists of a weaker or shorter testing stimuli immediately followed by a stronger masking stimulus of the same type. The stimuli types include visual inputs such as LED flash (Taylor and McCloskey 1996), target's

shape (Klotz and Wolff 1995), tactile/somatosensory inputs such as electrical shock (MacIntyre and McComas 1996) and auditory inputs (Kallman and Massaro 1979). Studies agreed that although subjects were not aware of the masked testing stimuli, their motor reaction time response (RT) to the masking stimuli were significantly shorter than RT response to the strong stimuli alone. Early neural activation has also been recorded from backward masking stimulus without awareness of the masked stimulus (James and Gauthier 2005; Noguchi and Kakigi 2005). In our study, perception of small perturbations was masked by a large background force, and our results were consistent with these previous masking studies that suggest that the motor response does not necessary rely on conscious perception.

Under the large background force condition, subjects responded differently to catch trials while they gradually adapted to the viscous force field. They deadapted quickly in response to catch trials when there was no background force, but not when there was a background force. This suggests that the subjects were not rapidly updating an internal model of the force field during side loading. We speculate that weaker perception in the side load condition impaired the confidence of the underlying error estimate. Alternately, the increased variance between consecutive trials related to the larger background force might have reduced the rate of internal model formation, although arguing against this possibility are previous studies that found that subjects adapt quickly to force fields with a randomly varying component (Scheidt et al. 2001b; Takahashi et al. 2001a, 2003).

Impedance control and the loading environment

Another key finding was that impedance control depended on the loading environment. To estimate limb impedance for each reach, we used catch trials in which the force field was unexpectedly toggled on or off. This differential change in force caused a differential change in the reaching trajectory, the magnitude of which must logically be governed by the limb impedance in the direction of the force field throughout the reach. Thus, the change in reaching trajectory is a marker for the limb impedance in the direction of the force field. Early in the reach, the change in trajectory is dictated primarily by the intrinsic muscle stiffness component of limb impedance, while later, reflex contributions to limb impedance may have occurred.

During reaching without the side load, limb impedance slowly increased with reaching practice. This slow increase may have been due to the unpredictable errors caused by the frequent application of randomly spaced catch trials. Previous research has suggested that the motor system increases its impedance in response to unpredictable or unstable force environments (Takahashi et al. 2001b; Franklin et al. 2003; Osu et al. 2003). In contrast, when impedance was already high during side loading due to the added stiffness from the elastic cords and the muscle stiffness/force dependence, the nervous system did not increase it further despite experiencing an identical catch trial protocol. Refraining from further increasing impedance in this condition makes sense from an energetic perspective: kinematic errors were relatively small due to the combined impedance of the elastic bands and loaded muscles, so that further voluntary increases in limb impedance would have a small effect though still being energetically costly. Thus, the nervous system appeared to use impedance control selectively depending on the background loading environment, in a way that likely contributed to the overall energy efficiency during adaptation.

The viscous force field we applied in this study was small, producing a peak magnitude perturbation of 3.3 N, and it might be argued that this small force led to the decreased perception or the failure to detect a change in impedance in some cases. However, the force field gain was large enough to produce significant direct effects and after effects with and without the background force, and to be perceived with a high degree of reliability without the background force. It was only when the background bungee force was added that perception became impaired; but in this case, the force field gain was the same, so this implicates the background force rather than a low force field gain as the reason for the decreased perception. Likewise, we detected a slow, trial-to-trial change in impedance when the background force was not present, indicating that the force field gain was large enough to cause such changes. The lack of such changes when the background force was present again implicates the background force for the change in impedance control properties, not the small force field gain.

Implications for mathematical models motor adaptation

Finally, we found that the parameters of two previously proposed mathematical models of force field adaptation changed significantly with the presence of the background force. The first model (Thoroughman and Shadmehr 2000; Scheidt et al. 2001a; Emken and Reinkensmeyer 2005) expressed motor adaptation in

terms of a linear difference equation that relates the kinematic error on one reach to the current force field (via coefficient b_1), previous error (via a_0), and previous force field (via b_0). The observed decrease in b_1 was consistent with the increase in limb/environment impedance experienced when the elastic cord was attached to the arm. However, the changes in a_0 and b_0 were more difficult to interpret: did they represent changes in the way that previous movement experiences affect future ones, or were they obligatory changes due to the altered mechanics of the reaching environment? We attempted to address this question by mapping the model parameters into a second model (Liu and Reinkensmeyer 2004; Emken and Reinkensmeyer 2005). This second model separated limb/environment dynamics from neural computations by assuming that the neural computation responsible for adaptation was an error-based learning law with a forgetting factor. We found that the forgetting factor decreased significantly during the side-loaded condition. Thus, the motor system acted as if it were seeking to more quickly decrease the force it applied, when the force regime in which it operated was more demanding.

We recently showed how the error-based learning law with a forgetting factor could be viewed as implementing an optimization procedure, in which the cost function to be minimized was the weighted sum of force and kinematic error (Reinkensmeyer et al. 2004). In other words, motor adaptation to a force field can be modeled as a tradeoff between allowing some ongoing kinematic error and generating enough force to cancel the force field. The forgetting factor determines the relative weighting of kinematic errors and exerted force in the cost function, with a smaller forgetting factor corresponding to a greater penalty for exerting more force. Within this framework, the decrease in forgetting factor with greater net loading observed in the present study would be viewed as an environmentally-triggered shift in the underlying cost function that can describe motor adaptation.

To summarize and conclude, then, the modeling results demonstrated how the model parameters vary significantly between the disparate force regimes studied here. Thus, comprehensive computational models of motor adaptation will likely need to include force-dependent parameters to accurately reproduce error dynamics. The need to consider force regimes in models of motor adaptation is consistent with the viewpoint that energy or effort considerations play a key role in shaping motor behavior.

References

Brewer BR, Fagan M, Klatzky RL, Matsuoka Y (2005) Perceptual limits for a robotic rehabilitation environment using visual feedback distortion. IEEE Trans Neural Syst Rehabil Eng 13:1–11

Burdet E, Osu R, Franklin DW, Milner TE, Kawato M (2001) The central nervous system stabilizes unstable dynamics by learning optimal impedance. Nature 414:446–449

Burdet E, Franklin DW, Osu R, Tee KP, Kawato M, Milner TE (2004) How are internal models of unstable tasks formed? In: IEEE 26th Annual international conference engineering in medicine and biology 6:4491–4494

Burdet E, Tee KP, Mareels I, Milner TE, Chew CM, Franklin DW, Osu R, Kawato M (2005) Stability and motor adaptation in human arm movements. Biol Cybern :1–13

Conditt MA, Gandolfo F, Mussa-Ivaldi FA (1997) The motor system does not learn the dynamics of the arm by rote memorization of past experience. J Neurophysiol 78:554–560

Donchin O, Francis JT, Shadmehr R (2003) Quantifying generalization from trial-by-trial behavior of adaptive systems that learn with basis functions: theory and experiments in human motor control. J Neurosci 23:9032–9045

Emken JL, Reinkensmeyer DJ (2005) Robot-enhanced motor learning: accelerating internal model formation during locomotion by transient dynamic amplification. IEEE Trans Neural Syst Rehabil Eng 13:33–39

Franklin DW, Osu R, Burdet E, Kawato M, Milner TE (2003) Adaptation to stable and unstable dynamics achieved by combined impedance control and inverse dynamics model. J Neurophysiol 90:3270–3282

Gandolfo F, Mussa-Ivaldi FA, Bizzi E (1996) Motor learning by field approximation. Proc Natl Acad Sci USA 93:3843–3846

Gomi H, Osu R (1998) Task-dependent viscoelasticity of human multijoint arm and its spatial characteristics for interaction with environments. J Neurosci 18:8965–8978

Goodale MA, Milner AD, Jakobson LS, Carey DP (1991) A neurological dissociation between perceiving objects and grasping them. Nature 349:154–156

Goodbody SJ, Wolpert DM (1998) Temporal and amplitude generalization in motor learning. J Neurophysiol 79:1825–1838

Goodbody SJ, Wolpert DM (1999) The effect of visuomotor displacements on arm movement paths. Exp Brain Res 127:213–223

Imanaka K, Kita I, Suzuki K (2002) Effects of nonconscious perception on motor response. Hum Mov Sci 21:541–561

James TW, Gauthier I (2005) Repetition-induced changes in BOLD response reflect accumulation of neural activity. Hum Brain Mapp 27:37–46

Johnson H, Haggard P (2005) Motor awareness without perceptual awareness. Neuropsychologia 43:227–237

Jones LA (1989) Matching forces: constant errors and differential thresholds. Perception 18:681–687

Jones LA, Hunter IW (1982) Force sensation in isometric contractions: a relative force effect. Brain Res 244:186–189

Kallman HJ, Massaro DW (1979) Similarity effects in backward recognition masking. J Exp Psychol Hum Percept Perform 5:110–128

Klassen J, Tong C, Flanagan JR (2005) Learning and recall of incremental kinematic and dynamic sensorimotor transformations. Exp Brain Res 164:250–259

Klotz W, Wolff P (1995) The effect of a masked stimulus on the response to the masking stimulus. Psychol Res 58:92–101

Liu J, Reinkensmeyer DJ (2004) Motor learning as an optimal combination of computational strategies. In: IEEE Engineering in Medicine and Biology Society Meeting, San Francisco, California, pp 4025–4028

MacIntyre NJ, McComas AJ (1996) Non-conscious choice in cutaneous backward masking. Neuroreport 7:1513–1516

McIntyre J, Mussa-Ivaldi FA, Bizzi E (1996) The control of stable postures in the multijoint arm. Exp Brain Res 110:248–264

Milner TE, Franklin DW (2005) Impedance control and internal model use during the initial stage of adaptation to novel dynamics in humans. J Physiol 567:651–664

Noguchi Y, Kakigi R (2005) Neural mechanisms of visual backward masking revealed by high temporal resolution imaging of human brain. Neuroimage 27:178–187

Osu R, Burdet E, Franklin DW, Milner TE, Kawato M (2003) Different mechanisms involved in adaptation to stable and unstable dynamics. J Neurophysiol 90:3255–3269

Pelisson D, Prablanc C, Goodale MA, Jeannerod M (1986) Visual control of reaching movements without vision of the limb. II. Evidence of fast unconscious processes correcting the trajectory of the hand to the final position of a double-step stimulus. Exp Brain Res 62:303–311

Reinkensmeyer DJ, Liu J, Emken JL, Bobrow JE (2004) The nervous system appears to minimize a weighted sum of kinematic error, force, and change in force when adapting to viscous environments during reaching and stepping. In: Symposium at the Society for Neuroscience Meeting, San Diego Convention Center. http://www.bme.jhu.edu/acmc/

Repp BH (2004) Comments on ''rapid motor adaptations to subliminal frequency shifts during syncopated rhythmic sensorimotor synchronization'' by Michael H. Thaut and Gary P. Kenyon [Hum Mov Sci 22:321–338, (2003)]. Hum Mov Sci 23:61–77; discussion 79–86

Rossetti Y, Rode G, Boisson D (1995) Implicit processing of somaesthetic information: a dissociation between where and how? Neuroreport 6:506–510

Scheidt RA, Dingwell JB, Mussa-Ivaldi FA (2001a) Learning to move amid uncertainty. J Neurophysiol 86:971–985

Scheidt RA, Dingwell JB, Mussa-Ivaldi FA (2001b) Learning to move amid uncertainty. J Neurophysiol 86:971–985

Shadmehr R, Brashers-Krug T (1997) Functional stages in the formation of human long-term motor memory. J Neurosci 17:409–419

Shadmehr R, Mussa-Ivaldi FA (1994) Adaptive representation of dynamics during learning of a motor task. J Neurosci 14:3208–3224

Shioiri S, Cavanagh P (1989) Saccadic suppression of low-level motion. Vision Res 29:915–928

Takahashi C, Scheidt R, Reinkensmeyer D (2001a) Impedance control and internal model formation when reaching in a randomly varying dynamical environment. J Neurophysiol 86:1047–1051

Takahashi CD, Scheidt RA, Reinkensmeyer DJ (2001b) Impedance control and internal model formation when reaching in a randomly varying dynamical environment. J Neurophysiol 86:1047–1051

Takahashi C, Nemet D, Rose-Gottron C, Larson J, Cooper D, Reinkensmeyer D (2003) Neuromotor noise limits motor performance, but not motor adaptation, in children. J Neurophysiol 90:703–722

Takahashi CD, Nemet D, Rose-Gottron CM, Larson JK, Cooper DM, Reinkensmeyer DJ (2006) Effect of muscle fatigue on internal model formation and retention during reaching with the arm. J Appl Physiol 100(2):695–706

Taylor JL, McCloskey DI (1996) Selection of motor responses on the basis of unperceived stimuli. Exp Brain Res 110:62–66

Thaut MH, Kenyon GP (2003) Rapid motor adaptations to subliminal frequency shifts during syncopated rhythmic sensorimotor synchronization. Hum Mov Sci 22:321–338

Thoroughman KA, Shadmehr R (2000) Learning of action through adaptive combination of motor primitives. Nature 407:742–747

Weber EH (1846) Der Tastsinn und Das Gemeingefuhl. Wagner's Hndworterbuch der Physiologie, vol 1/2, pp 481–588

Willingham D (2001) Becoming aware of motor skill. Trends Cogn Sci 5:181–182